Electrochemical deposition of 5,10,15,20-tetrakis-(4-sulphonatophenyl) porphyrin and its Co(II) derivative at a gold microelectrode array

Karolien De Wael [*],[1], Annemie Adriaens, Eduard Temmerman

Ghent University, Department of Analytical Chemistry, Krijgslaan 281 S12, B-9000 Ghent, Belgium

Abstract

This paper describes the fabrication and surface modification of gold microelectrode array structures. The modification is done by continuous cycling of the electrode array in a pH 12 buffer solution containing 8.01 mmol L^{-1} 5,10,15,20-tetrakis-(4-sulphonatophenyl)porphyrin tetrasodium salt (H$_2$TSPor). Incorporation of gold ions in the ligand during the potential cycling of the gold electrode is assumed. Only ring processes appear in the current potential curves, which do not change with scan number, indicating a fast adsorption. A second modification was performed through the electrodeposition of 5,10,15,20-tetrakis-(4-sulphonatophenyl)porphyrin Co(II) (CoTSPor) at a gold micro-electrode array.
© 2005 Elsevier B.V. All rights reserved.

1. Introduction

Porphyrins are widespread compounds in nature. They are important for several mechanisms in life: they catalyse enzymatic reactions and are, for instance, responsible for the oxygen transport in the human body [1]. The major characteristics of the porphyrin ring are its thermal and chemical stability, coupled with its extensive redox chemistry. The aromatic ring structure can be electrochemically oxidised and/or reduced [2].

Porphyrins have attracted wide research interest, including that of electrochemists, because of their ability to act as electron transfer mediators. As a result the charge transfer kinetics of the oxidation (or reduction) of some molecules, e.g. sodium dithionite, can be increased by modifying bare electrodes with porphyrins [3].

The use of electrodes with dimensions of micrometer range increased appreciably at the end of the seventies [4–6]. In contrast to electrodes of conventional dimensions, the measured current is considerably lower. As a result, the ohmic IR drop, even in organic solvents with high resistance, can often be kept sufficiently low [7–10] and voltammetric experiments can be performed with a specific 'low current' module. On the other hand, a better resolution and lower detection limits are obtained with microelectrodes and array structures because of the enhanced mass transport of electroactive species from radial diffusion [11,12].

The fabrication of microelectrodes and array structures is well documented in literature [13–15]. Random assemblies of microelectrodes (RAM) are good enough for analytical purposes since calibration curves will be used for the analytical application.

This paper describes, an easy way to construct microelectrode arrays as well as the modification of the array structure by electrodeposition of 5,10,15,20-tetrakis-(4-sulphonatophenyl)porphyrin tetrasodium salt (H$_2$TSPor). The adsorption at a gold electrode array structure in a pH 12 buffer solution, induced by potential cycling, is the subject of this article. This method is further called electrodeposition. A continuous potential cycling of the electrode between two potentials in a H$_2$TSPor solution can lead to a modification of the bare electrode. By measuring the current as a function of potential, it is possible to follow the adsorption process in situ. Characterisation of the modified electrodes is done by electrochemical and spectroscopic methods, including Raman spectroscopy. The electrodeposition of CoTSPor, Co(II) incorporated into the ligand, onto a gold macro electrode has been already described [16]. It was found that this deposition is initially controlled by kinetic parameters leading to a nearly 100% coverage of the

[*] Corresponding author. Tel.: +32 9 264 48 20; fax: +32 9 264 49 60.
E-mail address: karolien.dewael@ugent.be (K. De Wael).
[1] Postdoctoral Fellow of the Research Foundation, Flanders (FWO, Vlaanderen).

electrode surface. This article also describes the adsorption of CoTSPor onto a gold array structure.

2. Experimental

2.1. Materials and methods

A saturated calomel reference electrode (SCE) with two compartments (radiometer) and a carbon counter electrode were used. Gold wire, used to construct the array structure, was obtained from Advent (UK). The gold array was pretreated by mechanical and electrochemical polishing. Before its first use the electrode surface was scoured briefly on SiC-emery paper 1200 grit to obtain a fresh surface. To smoothen this relatively rough surface it is further subjected to sequential polishing on polishing cloth covered with alumina (Buehler) powder of 1, 0.3 and 0.05 μm particle size for, respectively 5, 10 and 20 min. To remove any adherent Al_2O_3 particles the electrode surface was rinsed thoroughly with doubly deionised water and cleaned in an ultrasonic bath (Branson 3210) for 2 min. Finally, the electrode was pretreated electrochemically by scanning between -0.15 and 1.29 V versus SCE in a 0.44 mol L^{-1} potassium nitrate solution for its characterisation and between -1.2 and 0.6 V versus SCE in a pH 12 buffer solution for its modification, until five subsequent scans were identical.

A PGSTAT20 potentiostat (ECO Chemie, Netherlands) controlled by GPES 4.9 software package running on a Pentium II computer (Eknadata) was used to record the voltammetric curves. The apparatus was extended with a low current module to perform voltammetry. Measurement of the pH of the solution was done with a Orion Benchtop pH-meter model 420A. The H_2TSPor and CoTSPor sodium salts were purchased from Porphyrin Systems (Lübeck, Germany). The buffer solution of pH 12 (Na_2HPO_4/NaOH), potassium nitrate (KNO_3) and potassium ferrocyanide ($K_4(Fe(CN)_6)$) were purchased from Riedel-de Haën. Prior to each experiment, pure nitrogen was bubbled through the cell solution for 20 min.

2.2. Fabrication of the array configuration

At right angles to the cross-section of a cylindrically shaped epoxy polymer, with a diameter of 21 mm and 1 cm length, 44 holes are drilled at 3 mm distance (Fig. 1). Through these holes, Au-wire with a diameter of 25 μm is woven. Two ways of preparing the array were used leading to a single woven and a double woven structure. Finally, the former will have 44 spots, the latter 88. On one side of the Au woven epoxy piece, a layer of Ag-cement enables the electrical contact between the gold wires and the brass holder. A plastic cylinder was pushed over the configuration and finally filled with epoxy monomer and hardener. After hardening, the top layer of the polymer was removed, in order to create an upper layer with Au spots on the surface. These 44 (single woven) or 88 (double woven) spots can act as electrode surfaces. All gold spots have a radius of 12.5 μm (491 $μm^2$ surface area).

3. Results and discussion

3.1. Characterisation of the array structure

The characteristics of both array structures, as well as the reproducibility of electrode surface regeneration, were examined by electrochemical methods. This characterisation was first carried out by multisweep cyclic voltammetry in 0.44 mol L^{-1} KNO_3. This test also served as a cleaning-activation procedure. Fig. 2 shows the cyclic voltammograms (10th scan) recorded at a 44-array structure and a 88-array structure, respectively with a 44 and 88 μm × 491 μm surface area. A well-defined oxidation wave at 0.16 V and reduction peak at 0.26 V versus SCE can be observed and are attributed to the oxidation of the gold surface and the reduction of the gold oxide formed during surface oxidation [17–20]. Both processes are adsorption phenomena, so a peak shaped voltammogram is obtained. As expected, the charge related to the reduction peak in curve 2 (0.441 μC) is two times larger than the charge associated with the 44-array (0.216 μC).
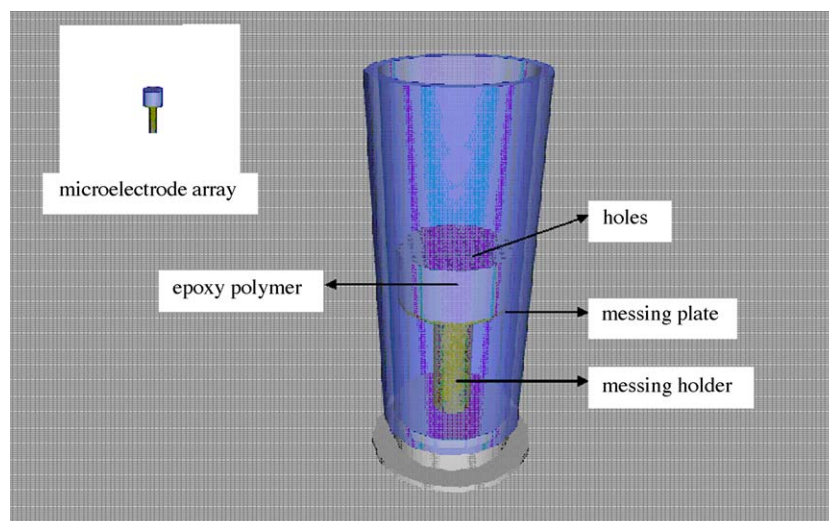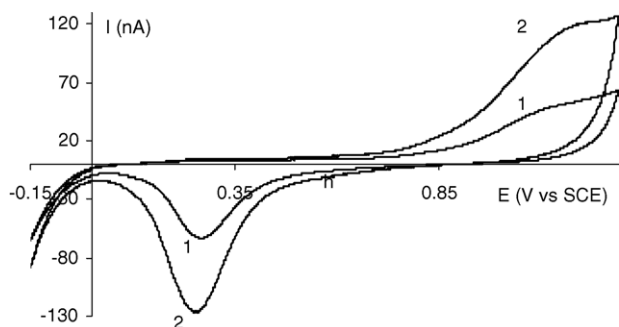

Fig. 1. Fabrication of the array structure.

Fig. 2. Current-potential curves obtained at a gold array electrode in a $0.44 \, mol \, L^{-1}$ KNO_3 solution at a scan rate of $50 \, mV \, s^{-1}$ and a temperature of 295.0 K. Curve 1 is recorded at the 44-array, curve 2 at the 88-array.

Reproducibility was examined after repeated cycles of cutting, polishing and rinsing, as described in the experimental section. Only small differences in cyclic voltammetric behaviour (maximum 8% variations in charges) between the measurements were obtained.

The diffusion characteristics of the array structures were studied in a solution of a reversible redox system. In Fig. 3 cyclic voltammetric curves are shown of the oxidation/reduction of the ferrocyanide/ferricyanide redox system at a gold 88-array. For the study of the oxidation of ferrocyanide

$$Fe(CN)^{4-}_{6aq} \rightarrow Fe(CN)^{3-}_{6aq} + e^- \qquad (1)$$
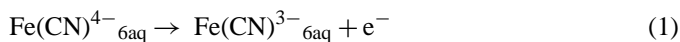
and the reduction of ferricyanide

$$Fe(CN)^{3-}_{6aq} + e^- \rightarrow Fe(CN)^{4-}_{6aq} \qquad (2)$$
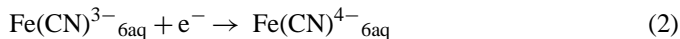
solutions of potassium ferrocyanide in $0.44 \, mol \, L^{-1}$ KNO_3 were employed. The concentration was varied between 2.5×10^{-5} and $1.1 \times 10^{-3} \, mol \, L^{-1}$ $Fe(CN)^{4-}_{6aq}$. Oxidation peak I_a and reduction peak I_c are the same as observed in Fig. 2 and can be attributed to the oxidation of the gold surface (I_a) and the reduction of the gold oxide layer (I_c) formed during process I_a. Since the formation of gold oxides results in a modification of the electrode surface, preference was given to the recording of cyclic voltammograms. By doing so, the gold surface will be identical before each addition of potassium ferrocyanide. Two other
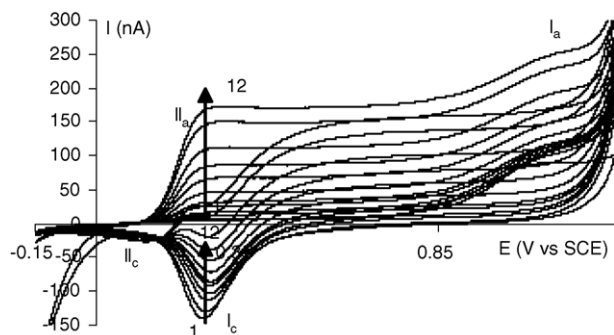
waves, II_a and II_c, are observed in Fig. 3 and can be attributed to oxidation of ferrocyanide (II_a, Eq. (1)) and reduction of ferricyanide (II_c, Eq. (2)) at the gold 88-array. In correlation with literature data [21], the half wave potential for both processes is 202 mV versus SCE. Processes II_a and II_c show a sigmoidally shaped transition to the diffusion limiting current (I_l) without any peaks. This is in agreement with the diffusion characteristics of planar microelectrodes, for which radial diffusion becomes dominant [13].

For sufficiently small values of the scan rate, the limiting current in cyclic voltammetry at an inlaid disc electrode (array structure) is given by

$$I_l = 4 \, p \, n \, r \, F \, D \, c \qquad (3)$$

with I_l the limiting current, p the number of spots in the array, n the number of electrons, r the radius of the electrode, F the Faraday's constant, D the diffusion coefficient and c the concentration of the electroactive species [13].

The influence of the concentration on the limiting current of process II_a was investigated to determine whether Eq. (3) is valid for the oxidation of potassium ferrocyanide at the gold array. In theory, the relationship between $\log I_l$ and $\log c$ should be linear and the slope of the relationship equal to 1. Fig. 4 shows this relationship for the oxidation of ferrocyanide depicted in Fig. 3 (gold 88-array, curve 1) and the data obtained for the gold 44-array (curve 2). Process II_a can be considered as resulting from a diffusion-limited steady-state process at an inlaid disc electrode (88 as well as 44-array) because the value of the $\log I_l$ versus $\log c$ slope is close to 1. Since there is a difference in number of electroactive spots, the ratio of both intercepts should be in theory 0.956 ($\log(176nrFD)/\log(352nrFD)$). The value of the intercept for curve 1 is 5.3207 and 5.5998 for curve 2. The ratio of these two values is 0.950, close to the theoretical value. Thus, the dependence on potassium ferrocyanide concentration follows Eq. (3) for both arrays.

3.2. Electrochemical deposition of H_2TSPor at a gold array structure

Fig. 5 shows some of the 100 cyclic voltammetric scans subsequently and continuously recorded at a gold 44-array in a pH 12 buffer solution (curve 1) and a solution containing

Fig. 3. Cyclic voltammograms of potassium ferrocyanide at a gold 88-array in a $0.44 \, mol \, L^{-1}$ KNO_3 solution at a scan rate of $50 \, mV \, s^{-1}$ and a temperature of 295.0 K for $Fe(CN)^{4-}_{6aq}$ concentrations of: (1) 0; (2) 5.00×10^{-5}; (3) 7.50×10^{-5}; (4) 1.00×10^{-4}; (5) 1.49×10^{-4}; (6) 2.00×10^{-4}; (7) 2.99×10^{-4}; (8) 3.99×10^{-4}; (9) 4.98×10^{-4}; (10) 5.97×10^{-4}; (11) 6.96×10^{-4}; and (12) $7.95 \times 10^{-4} \, mol \, L^{-1}$.
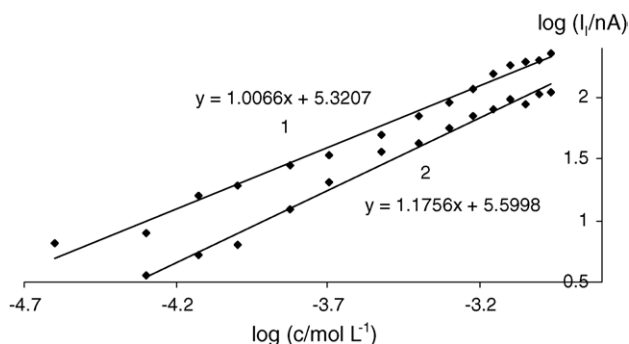

Fig. 4. Relationship between $\log I_l$ and $\log c$ for the oxidation of ferrocyanide at the gold 88-(1) and the gold 44-array (2).
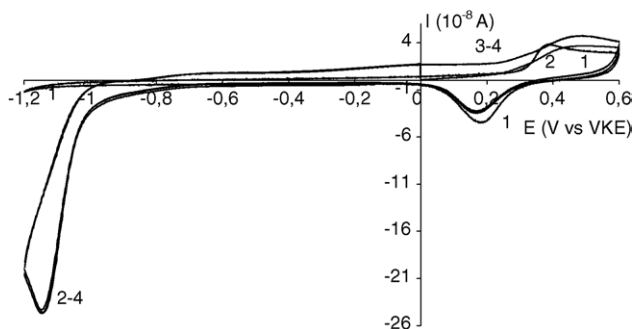
Fig. 5. Current-potential curves recorded at a gold disc electrode in a pH 12 buffer solution in the absence (curve 1) and presence (curves 2–4) of 8.01×10^{-3} mol L^{-1} H$_2$TSPor at a scan rate of 50 mV s^{-1} and a temperature of 298.0 K as a function of scan number. Scan numbers are (2) 2; (3) 40; and (4) 100.

8.01×10^{-3} mol L^{-1} H$_2$TSPor (curves 2–4). The peaks corresponding to the oxidation of the gold surface (A_a) and the reduction of the gold oxide formed during surface oxidation (A_c) [17–20], decrease when the electrode potential is cycled in a H$_2$TSPor solution. This is a first indication of adsorption of H$_2$TSPor onto the gold array structure, as covering the gold surface with H$_2$TSPor prevents its oxidation and subsequent reduction. The decrease of the gold oxidation and reduction processes is relatively small and as a result the amount of adsorbed H$_2$TSPor probably is quite low. There is only a small shift in peak potential during the decrease of signals A_a and A_c, thus these peaks are attributed to the gold processes only. The charge under the peak associated with the gold reduction (A_c) of scan 100 recorded in a H$_2$TSPor solution (curve 4) compared to the charge of the same reduction process in curve 1 (in the absence of H$_2$TSPor), leads to a coverage of circa 30%.

The cyclic voltammetric scans do not change with scan number, indicating a fast adsorption of H$_2$TSPor on the gold electrode. In comparison with the adsorption of MTSPc's on gold [22], there is no reorganisation of the adsorbed layer, resulting in a stable cyclic voltammogram. Due to the fact that four benzyl groups of the H$_2$TSPor molecule are perpendicularly oriented towards the ring structure; no reorganisation is possible in which columnar aggregates are formed.

Fig. 6 shows the cyclic voltammetric behaviour of different H$_2$TSPor concentrations at a gold electrode in a pH 12 buffer solution. As there is no central metal ion, only oxidation or reduction processes of the ligand structure are possible. All peaks observed in Figs. 5 and 6 can thus be explained as ring processes of CoTSPor present in solution. So, these processes are diffusion-controlled reactions. A well-defined reduction peak at -1.13 V versus SCE and two well-defined oxidation peaks at circa -0.5 and 0 V versus SCE can be observed, attributed to the reduction and oxidation of the ring structure. The relationship between peak currents and concentration of H$_2$TSPor is linear and the correlation coefficient was never smaller than 0.993. These peaks are too high to be explained by the reduction or oxidation of adsorbed H$_2$TSPor only. It is assumed that they result from an electrocatalytic reaction of H$_2$TSPor in solution. This is confirmed by the fact that these peaks disappear when
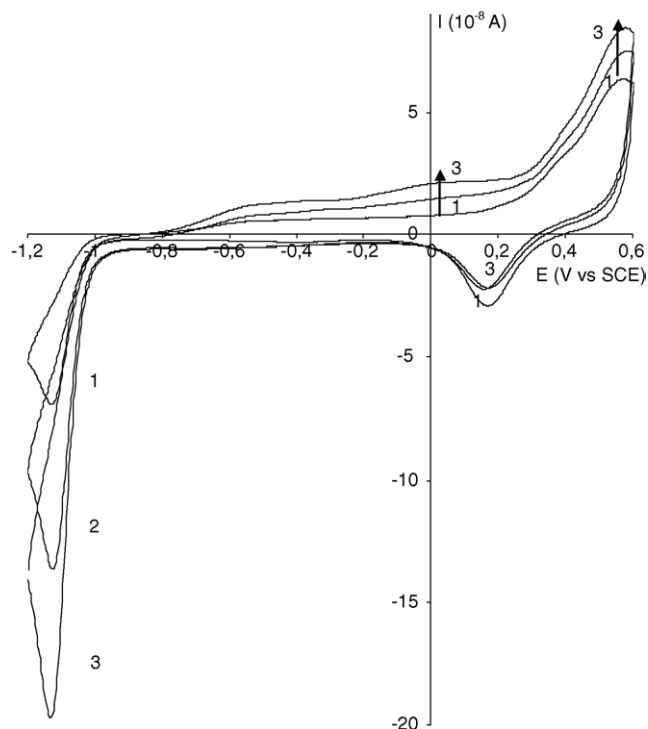

Fig. 6. Current-potential curves recorded at a gold disc electrode in a pH 12 buffer solution containing: 2.09 (1); 4.17 (2); and 6.26×10^{-3} (3) mol L^{-1} of H$_2$TSPor at a scan rate of 50 mV s^{-1} and a temperature of 298.0 K (10th scan).

the H$_2$TSPor modified electrode is scanned in a pH 12 buffer solution in the absence of H$_2$TSPor in solution. The first step in the electrocatalytic reduction reaction at -1.13 V versus SCE is supposed to be the ring reduction of adsorbed H$_2$TSPor. The next step is the reduction of H$_2$TSPor present in solution at this modified electrode.

The Raman spectroscopic analysis of a H$_2$TSPor modified gold electrode (gold electrode cycled in a 8.01×10^{-3} mol L^{-1} H$_2$TSPor solution during 100 scans) shows identical Raman bands compared to the Raman spectrum of a CoTSPor modified electrode, which is shown and explained in literature [16]. In addition, the positions and bandwidth of the most intense Raman bands are similar to those of the pure crystalline substances (1528, 1451, 748 and 681 cm^{-1}) [16]. Important to note is that the Raman spectrum of the H$_2$TSPor modified gold electrode is more similar to the spectrum of CoTSPor than to that of H$_2$TSPor powder. For the Raman spectra of CoTSPor and H$_2$TSPor is refered to literature data [4,22]. The similarity of the spectra of a H$_2$TSPor modified gold electrode and that of a CoTSPor modified electrode indicates the incorporation of gold atoms into the porphyrin ligand structure. This phenomenon is already described for Ag incorporation into a porphyrin structure during an anodization step [23] but was never observed for gold. Therefore it is assumed that a AuTSPor layer is formed onto the gold electrode. Because of the similarities between the Raman spectrum of a modified electrode and the spectrum of the corresponding powder, physisorption is responsible for the interaction between surface and molecules.
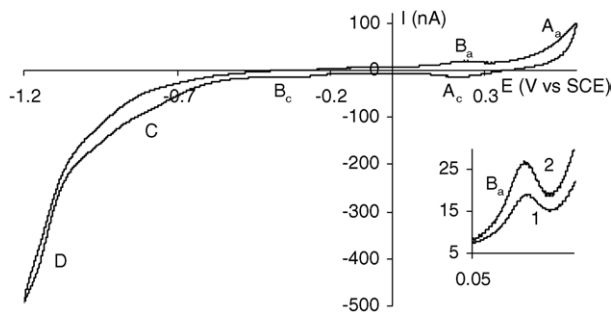
Fig. 7. Current-potential curve recorded at a gold 44-array in a pH 12 buffer solution after hundred scan cycling in a 7.95 mmol L^{-1} CoTSPor solution at a scan rate of 50 mV s^{-1}. Inset: oxidation of Co(II) at a gold 44-array (1) and at a gold 88-array (2).

3.3. Electrochemical deposition of CoTSPor at a gold array structure

The electrodeposition of 5,10,15,20-tetrakis-(4-sulphonato-phenyl)porphyrin Co(II), tetrasodium salt (CoTSPor) at gold macroelectrodes in a pH 12 buffer solution has been the subject of intensive investigation [16]. It was found that this deposition is initially controlled by kinetic parameters leading to a nearly 100% coverage of the electrode surface in which the CoTSPor molecules form a chaotic multilayer. After this initial stage, the adsorption is completed and followed by a slow reorganisation of the chaotic multilayer resulting in a thermodynamic more stable configuration (aggregation of CoTSPor molecules). A hypothesis regarding the electrodeposition of CoTSPor was based on the electrochemical observations made while following the current-potential behaviour as a function of scan number and CoTSPor concentration [16].

In this study the electrochemical behaviour of CoTSPor at a gold microelectrode array in alkaline solution is described. A continuous potential cycling of the gold 44-array between two potentials (−1.2 and 0.6 V versus SCE) in a 7.95 mmol L^{-1} CoTSPor pH 12 buffer solution at a scan rate of 50 mV s^{-1} leads, as is the case for a macroelectrode, to a modification of the gold spots. Fig. 7 represents the cyclic voltammetric curve obtained after hundred scans at a gold 44-array. Peaks due to the Co(III)$_{ads}$/Co(II)$_{ads}$ redox system (B_a and B_c) and to the ring oxidation and reduction of CoTSPor in solution (C and D) are identified as well as peaks due to gold oxidation and gold oxide reduction (A_a and A_c). As one can observe, the electrochemistry of the ligand is different from the CoTSPor-electrochemistry. The inset of Fig. 7 shows that the adsorption processes B_a, which represents the oxidation of Co(II)$_{ads}$ with formation of Co(III)$_{ads}$, is dependent on the dimensions of the array. The more gold spots at the array structure, the more CoTSPor that can be deposited on the surface. The charge under this peak, measured at the gold 44-array, is equal to 1.44×10^{-8} C (curve 1), nearly half of the value of the charge measured at the gold 88-array, 2.84×10^{-8} C (curve 2). These charges correspond to a CoTSPor coverage of 1.57×10^{-11} mol cm^{-2} (44-array) and 3.10×10^{-11} mol cm^{-2} (88-array). When the modified electrode is brought into a fresh buffer solution, peaks attributed to the adsorbed CoTSPor (B_a and B_c) are still present in the
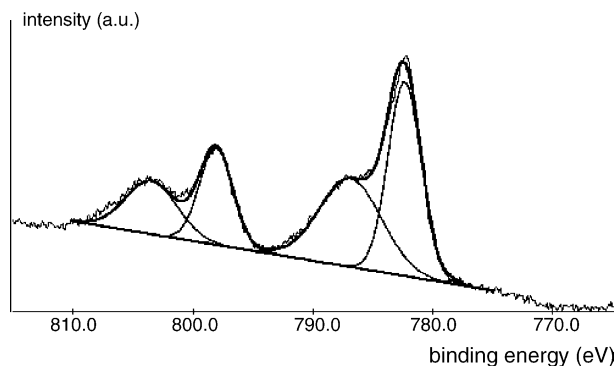

Fig. 8. The Co 2p XPS spectrum for a modified electrode after 100 scans in CoTSPor. The dark line represents the curve fit.

voltammetric curves and prove the formation of an adsorbed CoTSPor layer at the gold array structures. X-ray photoelectron spectroscopic analysis of the modified electrode was carried out, first of all to prove the adsorption by detecting the cobalt atom and secondly to confirm the value of the coverage. Fig. 8 shows the Co2p XPS-spectrum of a CoTSPor modified electrode. The dark line is the fitted curve. The cobalt 2p$_{1/2}$ and 2p$_{3/2}$ signals are present and give evidence of the deposition. The doublet separation is typical for an oxidized state, +II. Based on the atomic concentrations a value of 99.8% can be calculated, taking into account the molecular size of the CoTSPor molecule.

4. Conclusion

The fabrication and characterisation of a gold microelectrode array structure is described in this paper. The electrochemical characterisation was done by cyclic voltammetry in 0.44 mol L^{-1} KNO$_3$ solution containing different concentrations of potassium ferrocyanide. The Fe(III)/Fe(II) redox system behaves reversibly and shows a sigmoidally shaped steady-state voltammetric response.

In addition, this article describes the modification of a gold array structure by porphyrin ligand (H$_2$TSPor). During the continuous potential cycling in a H$_2$TSPor solution only ring processes could be observed and it was assumed, based on Raman analysis of the modified electrode, that a AuTSPor layer is formed. The produced gold array structures were also modified by continuous potential cycling in a 7.95 mmol L^{-1} CoTSPor solution. The peaks observed during the deposition can be attributed to reactions of the Co(III)/Co(II) redox system or the catalytic ring oxidation and reduction of CoTSPor. This modified gold array structure is expected to be a useful tool for electrocatalysis and electroanalysis.

References

[1] K.M. Kadish, K.M. Smith, R. Guilard, The Porphyrin Handbook, Academic Press, 2000.

[2] C.C. Leznoff, A.B.P. Lever, Phthalocyanines, Properties and Applications, vol. 3, VCH, Weinheim, 1993.

[3] K. De Wael, P. Westbroek, E. Temmerman, Electroanalysis 17 (2005) 263.

[4] R.N. Adams, Anal. Chem. 48 (1976) 1126A.

[5] J.L. Ponchon, R. Cespuglio, M. Gonon, M. Jouvet, J.F. Pujol, Anal. Chem. 51 (1979) 1483.

[6] R.M. Wightman, Anal. Chem. 53 (1981) 1125A.

[7] K.R. Wehmeyer, M.R. Deakin, R.M. Wightman, Anal. Chem. 57 (1985) 1913.

[8] J. Newman, J. Electrochem. Soc. 117 (1970) 198.

[9] A.M. Bond, M. Fleischmann, J. Robinson, J. Electroanal. Chem. 168 (1984) 299.

[10] A.M. Bond, M. Fleischmann, J. Robinson, J. Electroanal. Chem. 172 (1984) 11.

[11] A.G. Ewing, M.A. Dayton, R.M. Wightman, Anal. Chem. 53 (1981) 1842.

[12] A.S. Baranski, J. Electrochem. Soc. 133 (1986) 93.

[13] R.M. Wightman, D.O. Wipf, in: A.J. Bard (Ed.), Electroanalytical Chemistry, vol. 15, Marcel Dekker, New York, 1989.

[14] W. Thormann, P. van den Bosch, A.M. Bond, Anal. Chem. 57 (1985) 2764.

[15] J. Cassidy, J. Ghoroghchian, F. Sarfarazi, J.J. Smith, S. Pons, Electrochim. Acta. 31 (1986) 629.

[16] K. De Wael, P. Westbroek, E. Temmerman, A. Adriaens, Electrochim. Acta 50 (2005) 4269.

[17] L.D. Burke, J.F. O'Sullivan, Electrochim. Acta 37 (1992) 585.

[18] L.D. Burke, W.A. O'Leary, J. Appl. Electrochem. 19 (1989) 758.

[19] R. Woods, in: A.J. Bard (Ed.), Electroanalytical Chemistry, vol. 9, Marcel Dekker, New York, 1976.

[20] R.S. Sirohi, M.A. Gensham, J. Electrochem. Soc. 116 (1969) 910.

[21] R.D. Lafleur, J.C. Myland, K.B. Oldham, Electroanalysis 2 (1990) 223.

[22] K. De Wael, P. Westbroek, P. Bultinck, D. Depla, P. Vandenabeele, A. Adriaens, E. Temmerman, Electrochem. Commun. 7 (2005) 87.

[23] T.M. Cotton, S.G. Schultz, R.P. Van Duyne, J. Am. Chem. Soc. 104 (1982) 6528.